

## Hierarchically Macroporous Cryogels of Polyisobutylene and Silica Nanoparticles

Deniz C. Tuncaboğlu and Oguz Okay\*

Department of Chemistry, Istanbul Technical University, 34469 Maslak, Istanbul, Turkey

Received November 19, 2009. Revised Manuscript Received January 19, 2010

Organic–inorganic hybrid materials attract particular interest because of their excellent mechanical properties. Here, we report the synthesis of hybrid cryogels consisting of interpenetrated polyisobutylene and silica networks. The gels were prepared by cross-linking of butyl rubber in cyclohexane containing silica nanoparticles using sulfur monochloride ( $S_2Cl_2$ ) as a cross-linking agent. The microstructure of the hybrid networks formed at subzero temperatures exhibits two generations of pores:  $10^1 \mu\text{m}$  sized large pores due to the cyclohexane crystals acting as a template during gelation and,  $10^{-1}$ – $10^0 \mu\text{m}$  sized small pores between the aggregates of the nanoparticles. The nanoparticles in hybrid cryogels accumulate within the large pores where cyclohexane crystals originally resided. Compared to the organogel networks with an elastic modulus of a few kPa, hybrid networks exhibit a modulus of elasticity around 300 kPa. Hybrid cryogels can be converted into organic cryogels by dissolving the silica component in aqueous hydrofluoric acid, while removing the polymer component by calcination results in porous silica networks with  $10^{-1} \mu\text{m}$  sized pores.

## Introduction

Cryogelation is a simple route for the preparation of macroporous gels exhibiting a fast response rate and a high degree of toughness.<sup>1–3</sup> This technique is based on the natural principle that sea ice is less salty than seawater, that is, rejection of solutes from the growing ice crystals.<sup>4</sup> As in nature, during the freezing of an aqueous monomer solution, the monomers and the initiator expelled from the ice concentrate within the channels between the ice crystals, so that the polymerization reactions only take place in these unfrozen liquid channels. After polymerization and after thawing of ice, a macroporous material is produced whose microstructure is a negative replica of the ice formed. Macroporous polymers formed by cryogelation have large pores in the range of  $10^1$ – $10^2 \mu\text{m}$  separated by dense pore walls due to the high monomer concentration in the actual reaction zones. Such materials allowing a fast liquid transport through the continuous macropores have a broadened range of applications, such as separation media, catalyst, supports, adsorbents, and filters.

Several groups have described the preparation of macroporous hydrogels by the cryogelation technique.<sup>5–10</sup> Recently, we applied this technique to the nonaqueous gelation systems to obtain macroporous gels with hydrophobic pore walls.<sup>11,12</sup> The starting material of the organogel was a linear polyisobutylene containing

small amounts of internal unsaturated groups (isoprene units), known as butyl rubber (PIB). It was shown that the dilute solutions of PIB in benzene or in cyclohexane with normal freezing temperatures of 5.5 and 6 °C, respectively, can easily be cross-linked using sulfur monochloride ( $S_2Cl_2$ ) as a cross-linking agent.<sup>11–13</sup> Reactions in frozen PIB solutions lead to the formation of superfast responsive macroporous organogels with aligned pore structure. The organogels can be compressed up to about 100% strain without any crack development, during which the total liquid inside the gel is removed.<sup>11</sup> Further, the compressed gel immediately swells in contact with good solvents to recover its original shape. Such organogels are suitable materials in many application areas, for example, as reusable oil sorbent for the removal of oil spills and polycyclic aromatic hydrocarbons from waters.<sup>14</sup>

The major drawback of PIB cryogels or, in general, of porous gels is their low modulus of elasticity and low durability. Since the inclusion of inorganic nanoparticles into polymers as fillers is frequently used to enhance their mechanical performances,<sup>15–20</sup> we investigated the properties of the organogels as a function of the amount of an inorganic filler. We have to mention that organic–inorganic hybrid aerogels with high porosities have been prepared before by freeze-drying of aqueous clay gels containing various polymers<sup>21–23</sup> or by chemical cross-linking of silica aerogels.<sup>24,25</sup> Moreover, nonaqueous freeze-drying technique using camphene-based slurries was also used to prepare inorganic

\*To whom correspondence should be addressed. E-mail: okayo@itu.edu.tr.

- (1) Lozinsky, V. I. *Russ. Chem. Rev.* **2002**, *71*, 489.
- (2) Lozinsky, V. I.; Galaev, I. Yu.; Plieva, F. M.; Savina, I. N.; Junguid, H.; Mattiasson, B. *Trends. Biotechnol.* **2003**, *21*, 445.
- (3) Okay, O. In *Smart Polymers. Applications in Biotechnology and Biomedicine*; Galaev, I., Mattiasson, B., Eds; CRC Press, Taylor & Francis Group: New York, 2007; Chapter 9, p 296.
- (4) Worster, M. G.; Wettlaufer, J. S. *J. Phys. Chem. B* **1997**, *101*, 6132.
- (5) Zhang, X.-Z.; Chu, C.-C. *Chem. Commun.* **2003**, 1446.
- (6) Ozmen, M. M.; Okay, O. *Polymer* **2005**, *46*, 8119.
- (7) Dinu, M. V.; Ozmen, M. M.; Dragan, E. S.; Okay, O. *Polymer* **2007**, *48*, 195.
- (8) Plieva, F.; Huiting, X.; Galaev, I. Yu.; Bergenstahl, B.; Mattiasson, B. *J. Mater. Chem.* **2006**, *16*, 4065.
- (9) Gutierrez, M. C.; Ferrer, M. L.; del Monte, F. *Chem. Mater.* **2008**, *20*, 634.
- (10) Kirsebom, H.; Mattiasson, B.; Galaev, I. Yu. *Langmuir* **2009**, *25*, 8426.
- (11) Ceylan, D.; Okay, O. *Macromolecules* **2007**, *40*, 8742.
- (12) Dogu, S.; Okay, O. *Polymer* **2008**, *49*, 4626.

- (13) Okay, O.; Durmaz, S.; Erman, B. *Macromolecules* **2000**, *33*, 4822.
- (14) Tuncaboğlu, D. C.; Dogu, S.; Karacik, B.; Yakan, S. D.; Okay, O. S.; Okay, O. *Environ. Sci. Technol.* **2009**, *43*, 3846.
- (15) Haraguchi, K.; Takehisa, T. *Adv. Mater.* **2002**, *14*, 1120.
- (16) Sanchez, C.; Julian, B.; Belleville, P.; Popall, M. *J. Mater. Chem.* **2005**, *15*, 3559.
- (17) Suzuki, T.; Endo, H.; Osaka, N.; Shibayama, M. *Langmuir* **2009**, *25*, 8824.
- (18) Guvendiren, M.; Heiney, P. A.; Yang, S. *Macromolecules* **2009**, *42*, 6606.
- (19) Lozinskii, V. I.; Savina, I. N. *Colloid J.* **2002**, *64*, 336.
- (20) Lozinsky, V. I.; Bakeeva, I. V.; Presnyak, E. P.; Damshkaln, L. G.; Zubov, V. P. *J. Appl. Polym. Sci.* **2007**, *105*, 2689.
- (21) Bandi, S.; Bell, M.; Schiraldi, D. A. *Macromolecules* **2005**, *38*, 9216.
- (22) Arndt, E. M.; Gawryla, M. D.; Schiraldi, D. A. *J. Mater. Chem.* **2007**, *17*, 3525.
- (23) Gawryla, M. D.; Liu, L.; Grunlan, J. C.; Schiraldi, D. A. *Macromol. Rapid Commun.* **2009**, *30*, 1669.

porous materials with interconnected pore channels.<sup>26–29</sup> In the present work, fumed silica nanoparticles of 16 nm in diameter were used as filler at various amounts. The gels were prepared by cross-linking of PIB in cyclohexane solutions in the presence of silica nanoparticles at various temperatures. As will be seen below, a remarkable enhancement in the mechanical properties of gels was observed after modification with silica particles. We also observed that the hybrid cryogels consisting of organic and inorganic components have two hierarchies of pore structure at the same time: large pores due to the frozen cyclohexane crystals acting as a template, and the other smaller pores in the interstices of the agglomerated nanoparticles.

## Experimental Section

**A. Materials.** Butyl rubber (Butyl 365, Exxon Chem. Co) used as the polymer component of hybrid gels contained 2.3 mol % isoprene units. It was dissolved in toluene followed by precipitation into methanol and drying at room temperature under vacuum to constant mass. Homogeneous solutions of butyl rubber (PIB) were prepared by dissolving PIB in cyclohexane for 1 day. The molecular weight and the radius of gyration of PIB were determined using a commercial multiangle light scattering DAWN EOS (Wyatt Technologies Corporation) instrument equipped with a vertically polarized 30 mW gallium–arsenide laser operating at  $\lambda = 690$  nm and 18 simultaneously detected scattering angles. The light scattering system was calibrated against a toluene standard. The scattered light intensities from PIB solutions in cyclohexane were recorded from angles  $\theta = 54^\circ$  to  $153^\circ$ . The refractive index increment  $dn/dc$  was determined using the same polymer solutions using a DAWN Optilab DSP instrument at 690 nm. The  $dn/dc$  value of PIB in cyclohexane was found to be  $0.068 \pm 0.005$  mL/g. From the scattering data recorded at various scattering vectors and PIB concentrations, the radius of gyration and the weight-average molecular weight of PIB were determined from the Zimm plot as  $38 \pm 6$  nm and  $1.0 (\pm 0.2) \times 10^6$  g/mol, respectively.

As the inorganic component of the organogels, fumed silica particles Aerosil R-972 (Evonik Industries) with a surface area of  $110 \pm 20$  m<sup>2</sup>/g and particle diameter of 16 nm were used. Approximately 70% of silanol groups on the silica surfaces were modified by dimethyldichlorosilane during its manufacture so that it is hydrophobic and could not be dispersed in water even if violently stirred. The cross-linking agent sulfur monochloride, S<sub>2</sub>Cl<sub>2</sub>, was purchased from Aldrich Co. Dispersions of Aerosil R-972 were prepared by dispersing the white powder at the preset concentrations in cyclohexane with vigorous stirring for 1 day. Cyclohexane, toluene, and methanol (all Merck grades) were used as the solvent for the solution cross-linking reactions, swelling, and deswelling agents, respectively.

**B. Synthesis of the Gels.** The gels were prepared by solution cross-linking technique at a PIB concentration of 5 w/v %. The amount of the cross-linker S<sub>2</sub>Cl<sub>2</sub> was also fixed at 10 mL/100 g PIB. Silica content of the reaction solutions was varied between 0 and 4 w/v %. Gelation solutions were prepared by mixing solutions of PIB and Aerosil R-972 under stirring for 5 min. The cross-linking reactions were initiated by addition of the cross-linker S<sub>2</sub>Cl<sub>2</sub> under rigorous stirring at 13 °C. Then the reaction

solutions were transferred into plastic syringes of 16 mm internal diameters. The cross-linking reactions were conducted both in a thermostatted room at 13 °C as well as in a freezer at predetermined temperatures between  $-2$  and  $-18$  °C for 3 days.

**C. Rheological Measurements.** Reaction solutions containing PIB and silica as well as the resulting gels were investigated using a rheometer (Gemini 150 Rheometer system, Bohlin Instruments) equipped with a Peltier device for temperature control. The upper plate (diameter 40 mm) was set at a distance of 500  $\mu$ m before the onset of the reactions, that is, during the induction period. During all rheological measurements, a solvent trap containing cyclohexane was used to minimize the evaporation. During the frequency sweep experiments, a strain amplitude of 1% was selected to ensure that the oscillatory deformation is within the linear regime.

**D. Characterization of Gels and Networks.** PIB gels were taken out of the syringes, and they were cut into specimens of approximately 10 mm in length. Each gel sample was placed in an excess of toluene at 20 °C, and toluene was replaced every other day over a period of at least 1 month to wash out the soluble polymer, silica nanoparticles, and unreacted cross-linker. The swelling equilibrium was tested by measuring the diameter of the gel samples by using an image analyzing system consisting of a microscope (XSZ single Zoom microscope), a CDD digital camera (TK 1381 EG), and a PC with the data analyzing system Image-Pro Plus. The swelling equilibrium was also tested by weighing the gel samples. In order to dry the equilibrium swollen gel samples, they were first immersed in methanol (poor solvent) overnight and then dried under vacuum. Then the dry gel samples were calcinated to remove the organic matter. Preliminary thermogravimetric analysis results showed that the PIB networks prepared in the absence of silica totally disappear if they are heated at 600 °C for 4 h. Therefore, all the calcination reactions were carried out under this condition. The gel fraction  $W_g$  defined as the amount of cross-linked (insoluble) polymer obtained from 1 g of PIB and the silica %, that is, the amount of silica bound to the cross-linked polymer in 100 mL of gel after preparation, were calculated as

$$W_g = \frac{m_{\text{dry}} - m_{\text{silica}}}{m_o c_p / 100} \quad (1a)$$

$$\text{silica \%} = \frac{m_{\text{silica}}}{m_o} \times 10^2 \quad (1b)$$

where  $m_{\text{dry}}$ ,  $m_{\text{silica}}$ , and  $m_o$  are the weights of the gel samples after drying, after calcination, and just after preparation, respectively, and  $c_p$  is the initial PIB concentration. The equilibrium volume and the equilibrium weight swelling ratios of the gels,  $q_v$  and  $q_w$ , respectively, were calculated as

$$q_v = (D/D_{\text{dry}})^3 \quad (2a)$$

$$q_w = (m/m_{\text{dry}}) \quad (2b)$$

where  $D$  and  $D_{\text{dry}}$  are the diameters of the equilibrium swollen and dry gels, respectively, and  $m$  and  $m_{\text{dry}}$  are the weights of gels after equilibrium swelling in toluene and after drying, respectively.

Uniaxial compression measurements were performed on both equilibrium swollen and dry gels in toluene. All the mechanical measurements were conducted in a thermostatted room of  $20 \pm 0.5$  °C. The stress–strain isotherms were measured by using an apparatus previously described.<sup>30,31</sup> The shear modulus  $G$  was determined from the initial slope of linear dependence,

(24) Zhang, G.; Dass, A.; Rawashdeh, A. M.; Thomas, J.; Counsil, J. A.; Sotiriou-Leventis, C.; Fabrizio, E. F.; Ilhan, F.; Vassilaras, P.; Scheiman, D. A.; McCorkle, L.; Palczar, A.; Johnston, J. C.; Meador, M. A.; Leventis, N. *J. Non-Cryst. Solids* **2004**, *350*, 152.

(25) Meador, M. A. B.; Fabrizio, E. F.; Ilhan, F.; Dass, A.; Zhang, G.; Vassilaras, P.; Johnston, J. C.; Leventis, N. *Chem. Mater.* **2005**, *17*, 1085.

(26) Araki, K.; Halloran, J. W. *J. Am. Ceram. Soc.* **2005**, *88*, 1108.

(27) Koh, Y.-H.; Song, J.-H.; Lee, E.-J.; Kim, H.-E. *J. Am. Ceram. Soc.* **2006**, *89*, 3089.

(28) Yoon, B.-H.; Koh, Y.-H.; Park, C.-S.; Kim, H.-E. *J. Am. Ceram. Soc.* **2007**, *90*, 1744.

(29) Yoon, B.-H.; Lee, E.-J.; Kim, H.-E. *J. Am. Ceram. Soc.* **2007**, *90*, 1753.

(30) Sayil, C.; Okay, O. *Polymer* **2001**, *42*, 7639.

(31) Gundogan, N.; Melekaslan, D.; Okay, O. *Macromolecules* **2002**, *35*, 5616.

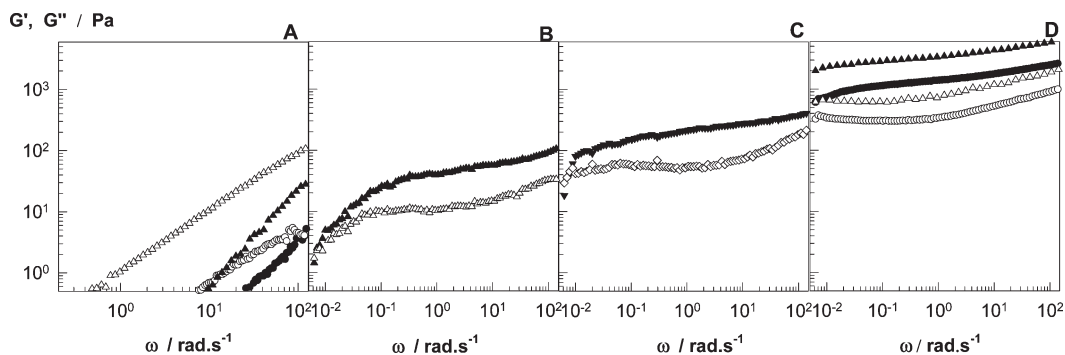


**Figure 1.** Elastic modulus  $G'$  (filled symbols) and viscous modulus  $G''$  (open symbols) shown as a function of the angular frequency  $\omega$  at 25 °C. (A) PIB solutions with 5 (circles) and 9% PIB (triangles). (B) 4% silica dispersion. (C) 5% PIB solution containing 4% silica. (D) PIB gels formed at 13 °C and at a PIB concentration of 5%. Silica = 0% (circles) and 4% (triangles).

$f = G(\alpha - \alpha^{-2})$ , where  $f$  is the force acting per unit cross-sectional area of the undeformed gel specimen and  $\alpha$  is the deformation ratio (deformed length/initial length).

The pore volume  $V_p$  of the networks was estimated through uptake of methanol of dry gels.<sup>32</sup> Since methanol is a nonsolvent for PIB, it only enters into the pores of the polymer networks.<sup>11</sup> Thus,  $V_p$  (mL pores in 1 g of dry polymer network) was calculated as

$$V_p = (m_M - m_{dry}) / (d_M m_{dry}) \quad (3)$$

where  $m_M$  is the weight of the network immersed in methanol after 2 h and  $d_M$  is the density of methanol.

Thermogravimetric analysis (TGA) of hybrid networks was performed on a Perkin-Elmer Diamond TA/TGA instrument with a temperature scan from 30 to 900 °C at a heating rate of 10 °C/min under nitrogen flow.

For the texture determination of dry gels, scanning electron microscopy studies were carried out at various magnifications between 10 and 30000 times (Jeol JSM 6335F field emission SEM). Prior to the measurements, network samples were sputter-coated with gold for 3 min using a Sputter-coater S150 B Edwards instrument. Environmental scanning electron microscope (ESEM) measurements were conducted on a XL30 ESEM-FEG/EDAX system (Philips). ESEM images were obtained at magnifications between 50 and 3000 times under varying pressure from 0.3 to 0.9 Torr. The pore sizes and the pore size distribution of the networks were determined by mercury porosimetry (Quantachrome Poremaster 60). This technique involves penetration of mercury, at known pressures, into the pores of dry polymer and is based on the Washburn relationship that the pressure required to force the mercury into the pores is inversely proportional to their radius.

In order to convert hybrid gels to organogels, dry hybrid network samples were immersed in an excess of 48% aqueous hydrofluoric acid (HF) for 1 week. Thereafter, the samples were first washed with water and then with methanol and finally dried under vacuum to constant mass.

## Results and Discussion

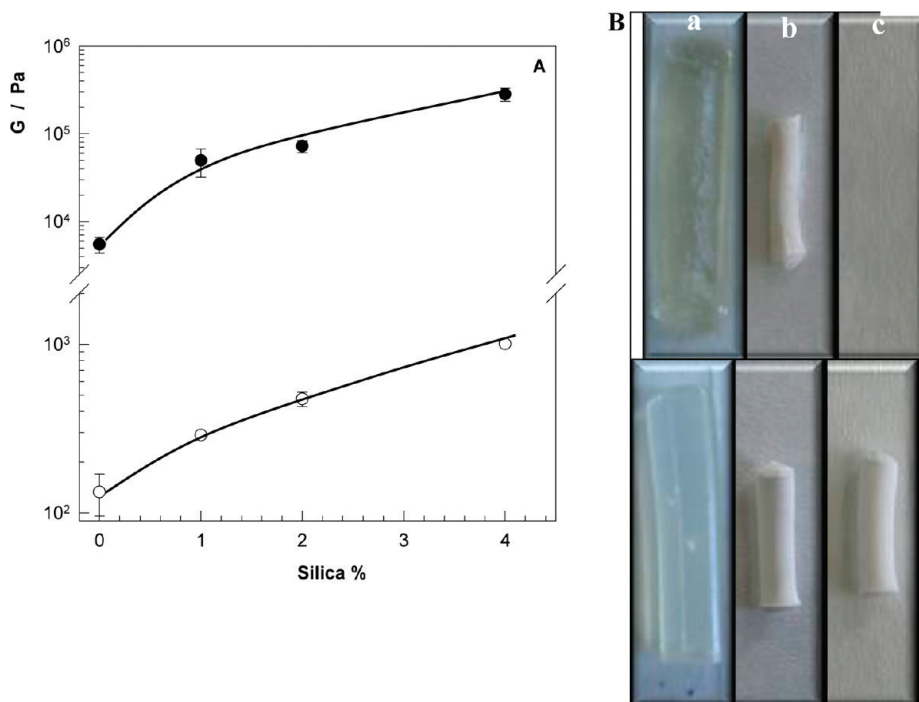
Hybrid organogels and cryogels were prepared by solution cross-linking of PIB in cyclohexane and in the presence of silica nanoparticles at various temperatures, both below and above the bulk freezing temperature of the reaction solution. We discuss the results of our experiments in four subsections. In the first subsection, rheological characteristics of the gelation solutions are presented. In the following subsections, the properties of hybrid gels of various silica contents are discussed and experimental observations are interpreted.

**A. Rheological Behavior of Silica Dispersions in PIB Solutions.** Before the characteristics of the hybrid gels are discussed, it may be instructive to illustrate the oscillatory response of the reaction solutions containing the polymer chains and silica nanoparticles. Figure 1A–C shows dynamic rheological behavior of PIB solutions with 5 and 9% PIB (A), 4% silica dispersion (B), and 5% PIB solution containing 4% silica particles (C). Here, the elastic modulus  $G'$  (filled symbols) and the viscous modulus  $G''$  (open symbols) of the solutions or dispersions are plotted against the angular frequency  $\omega$ . PIB solutions exhibit a liquidlike response typical for a semidilute polymer solution; that is,  $G''$  exceeds  $G'$  at low frequencies while there is a crossover between  $G'$  and  $G''$  at a high frequency. In contrast, the 4% silica dispersion in cyclohexane is a viscoelastic gel above a frequency of  $10^{-2}$  s. This indicates formation of a colloidal gel in which the silica units are connected together into a volume-filling network structure. Further, the 4% silica dispersion in PIB solution is also a viscoelastic gel exhibiting higher dynamic moduli compared to the silica dispersions in the absence of PIB. Frequency sweep tests also showed that both  $G'$  and  $G''$  increase with increasing silica content from 1 to 4% (Supporting Information Figure S1), indicating that the elastic properties as well as the extent of energy dissipation increase with increasing amount of silica in the dispersions. Thus, silica particles interact between themselves due to van der Waals forces and depletion forces (in the presence of PIB) to form a physical network in cyclohexane, while the polymer segments adsorbed on the particle surfaces increase further its viscous and elastic properties.

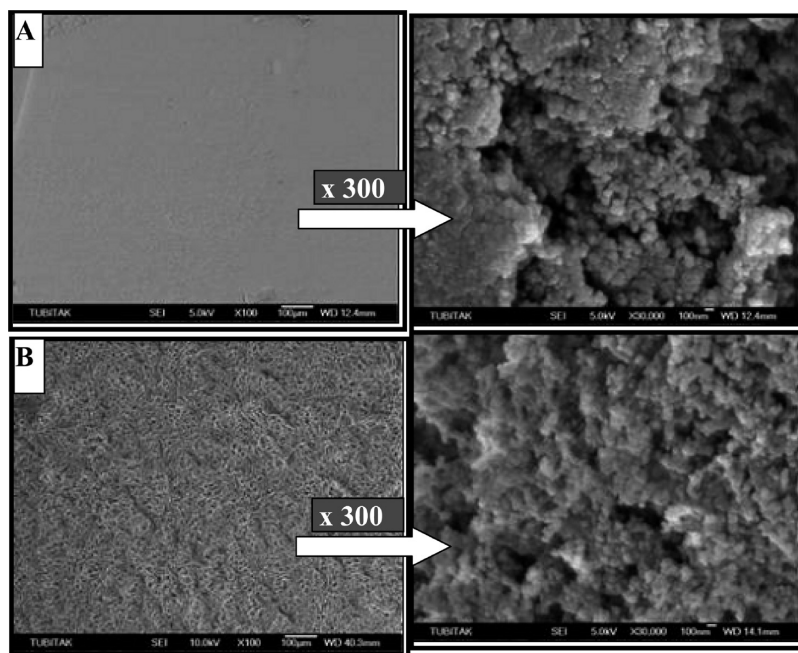
**B. Hybrid Gels.** PIB solutions containing nanoparticles were subjected to the cross-linking reactions using  $S_2Cl_2$  as the cross-linking agent at temperatures between 13 and –18 °C. To compare the dynamic moduli of gels with those of the starting reaction solutions, we first conducted frequency-sweep tests on hybrid gels just after their preparation at 13 °C. The results are given in Figure 1D for gels with 0 and 4% silica. Comparison reveals that both  $G'$  and  $G''$  increase after the cross-linking reactions as well as after inclusion of the nanoparticles in the organogels. PIB solution after cross-linking becomes a gel with a modulus of elasticity  $G'$  of about 1 kPa at  $\omega = 6.3 \text{ rad} \cdot \text{s}^{-1}$ , while addition of 4% silica further increases  $G'$  to 4 kPa. Moreover,  $G'$  increases with increasing frequency due to the contribution of the silica network to the elasticity of the polymer matrix at short time scales.

Figure 2A shows the shear modulus  $G$  of gels formed at –18 °C at various silica contents. The measurements were conducted using uniaxial compression tests on gel samples in the dry and in the swollen states in toluene. The moduli of dry and swollen gels significantly increase with increasing silica content and become

(32) Okay, O. *Prog. Polym. Sci.* **2000**, *25*, 711.



**Figure 2.** (A) Shear modulus  $G$  of dry (filled symbols) and equilibrium swollen gels in toluene (open symbols) shown as a function of silica content. Gel preparation temperature =  $-18^\circ\text{C}$ . (B) Optical images of gels formed at  $-18^\circ\text{C}$  in the presence of 0 (upper panel) and 4% silica nanoparticles (bottom panel). Images were taken from gel samples after equilibrium swelling in toluene (a), after drying (b), and after calcination at  $600^\circ\text{C}$  (c). Note that the gel sample without silica completely disappears after calcination.



**Figure 3.** SEM images of gel networks formed at  $13^\circ\text{C}$  (A) and  $-18^\circ\text{C}$  (B) in the presence of 4% silica. Scale bars are  $100\ \mu\text{m}$  (left) and  $100\ \text{nm}$  (right).

300 and 1 kPa at 4% silica, respectively. More than 1 order of magnitude increase in the modulus of gels with the incorporation of the nanoparticles is due to the interpenetration of the silica and PIB networks in hybrid gels. Figure 2B shows optical images of the gels formed at  $-18^\circ\text{C}$  at three different states: (a) equilibrium swollen state in toluene, (b) dry state, and (c) after calcination at  $600^\circ\text{C}$ . The equilibrium weight ( $q_w$ ) and volume swelling ratios ( $q_v$ ) of the gels in toluene were  $20 \pm 5$  and  $7 \pm 2$ , respectively,

independent of the preparation temperature, but they decreased slightly with increasing silica content due to the cross-linking effect of the nanoparticles. Thermogravimetric analysis experiments on the gel networks showed that the PIB network started pyrolyzing at  $300^\circ\text{C}$  and was completely pyrolyzed by  $600^\circ\text{C}$ , leaving silica particles (Supporting Information Figure S2). As seen in Figure 2B, the gel without silica completely disappears after calcination due to the removal of the organic matter at this

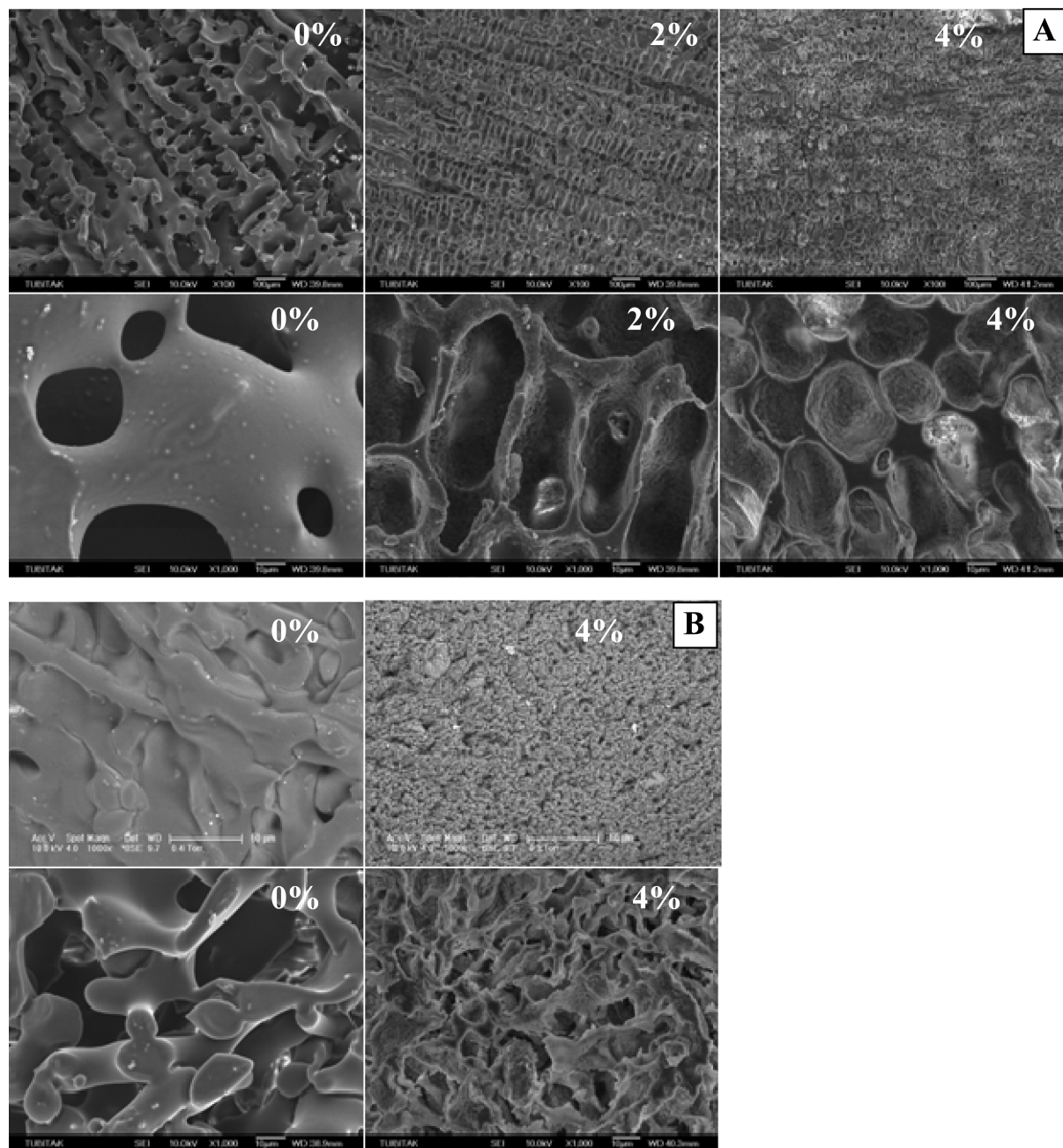


**Figure 4.** SEM and ESEM images (third row) of gel networks with various silica contents indicated. Gel preparation temperature =  $-2\text{ }^{\circ}\text{C}$  (A) and  $-18\text{ }^{\circ}\text{C}$  (B).

temperature. However, the gel containing silica particles retains its shape, indicating that the three-dimensional silica network formed in cyclohexane, as observed by the rheological measurements (Figure 1), is preserved in the dry state. We have to mention that the silica network obtained after calcination was extremely fragile and can be broken down into powder using hand pressure. For all hybrid gels formed between  $-2$  and  $-18\text{ }^{\circ}\text{C}$ , calculations showed that both the polymer and the silica amounts in the extracted gels are close to those in the reaction solutions (Supporting Information Table S1), indicating that PIB and silica are incorporated into the network structure.

Figure 3 shows typical scanning electron microscope (SEM) images of hybrid gel networks with 4% silica at two different magnifications. The preparation temperature of gels is  $13\text{ }^{\circ}\text{C}$  (A) and  $-18\text{ }^{\circ}\text{C}$  (B). At lower magnification, no pores are seen in the  $13\text{ }^{\circ}\text{C}$  gel network, indicating that the gel is homogeneous at this

size scale, while regular pores of sizes  $10^1\text{ }\mu\text{m}$  are visible in the  $-18\text{ }^{\circ}\text{C}$  gel network. These pores are typical for macroporous networks created by the cryogelation technique.<sup>11,12</sup> Thus, the apparently frozen state of the reaction system at  $-18\text{ }^{\circ}\text{C}$  produces macropores that are templated from the spaces occupied by the cyclohexane crystals. Under higher magnification, however, both gels exhibit similar morphologies consisting of aggregates of spherical silica particles with submicrometer-sized interstices forming the pore structure. The results demonstrate that the microstructure of the gel network formed at  $-18\text{ }^{\circ}\text{C}$  consists of two generations of pores:  $10^1\text{ }\mu\text{m}$  sized large pores due to the cyclohexane template and  $10^{-1}$ – $10^0\text{ }\mu\text{m}$  sized small pores between the aggregates of the nanoparticles.

**C. Large Pores in Hybrid Gels.** Pores of  $10^1\text{ }\mu\text{m}$  size in hybrid gels appear in regions where cyclohexane crystals located during cryogelation. These pores will in the following be designated

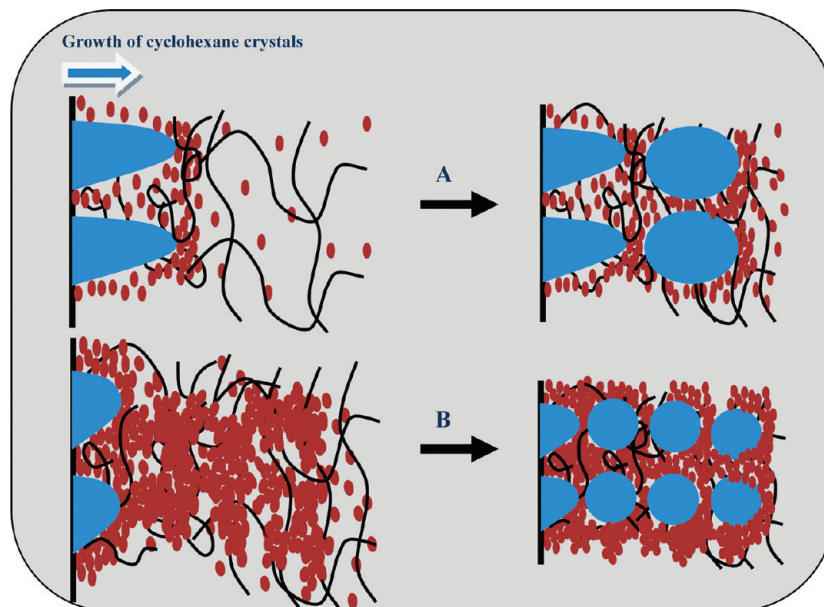


**Figure 5.** Cartoon demonstrating the growth of the cyclohexane crystals during cryogelation reactions in the presence of silica particles at a low (A) and high (B) concentration.

as large pores, while those between the nanoparticles and their agglomerates will be called small pores. SEM and environmental scanning electron microscope (ESEM) images in Figure 4 illustrates how the size and the shape of the large pores vary depending on the amount of silica and on the gel preparation temperature. Silica contents of the gel networks are indicated in the figure.

The images in Figure 4A were taken from gels formed at  $-2\text{ }^{\circ}\text{C}$  at two different magnifications. The general trend is that the size of the pores decreases while their number increases with increasing silica content and, simultaneously, the pores become increasingly regular. The decrease in the pore size is due to the accumulation of the silica particles in the inner part of the pore walls, as can be observed in the enlarged images (second row in Figure 4A). SEM images of the hybrid networks of various silica contents indicated that the larger the silica content, the thicker the thickness of the silica layer on the pore walls (Supporting Information Figure S3). At 4% silica, the nanoparticles partly fill the pores and convert them into concave-shaped pores, indicating that frozen cyclohexane had been accumulated during cryogelation in the hollow portion of these pores (Figure 4A, bottom right image). The results thus demonstrate that, in hybrid gels, the silica particles are segregated from the polymer and they accumulate within the large pores where cyclohexane crystals originally resided. Similar results were also observed for gels prepared at  $-18\text{ }^{\circ}\text{C}$ . ESEM and SEM images given in Figure 4B illustrate the decrease of the pore size and accumulation of the silica particles in the pores with the addition of silica.

The total volume of pores  $V_p$  estimated from the methanol uptake of dry networks was found to be largely insensitive to the gel preparation temperature between  $-2$  and  $-18\text{ }^{\circ}\text{C}$  as well as to the silica content. The average of the total pore volumes  $V_p$  of 16 different gel networks prepared at  $-2$ ,  $-7$ ,  $-10$ , and  $-18\text{ }^{\circ}\text{C}$  with 0, 1, 2, and 4% silica was found to be  $2.5 \pm 0.7\text{ mL/g}$ , which slightly increased with decreasing temperature, or with increasing silica content. This suggests that the addition of silica only affects the size and the shape of the pores without changing their cumulative volumes. Comparison of the morphologies of hybrid gels also shows that those prepared at  $-2\text{ }^{\circ}\text{C}$  have a regular porous structure consisting of hexagonal and spherical pores at 2

and 4% silica, respectively (Figure 4). The regularity of the porous structure is largely destroyed by decreasing the gelation temperature to  $-18\text{ }^{\circ}\text{C}$ . A similar behavior was recently observed in the absence of silica particles and originates from the increasing rate of freezing of the reaction solution as the temperature is decreased and also is due to the collapse of the pores formed at low temperatures.<sup>11,12</sup>

We may explain the decrease of the pore size with increasing silica content as well as segregation of silica from the polymer according to the following scenario (Figure 5): Because of the poor conductivity of the reaction solution, a temperature gradient is formed in the radial direction and thus freezing of cyclohexane starts from the surface of the cylindrical reactor, which is in contact with the cooling liquid. During freezing, the silica particles, the polymer chains, and the cross-linker molecules are pushed by the advancing freezing front so that the concentration of the unfrozen dispersion increases. This pushing of the solutes also results in a concentration gradient within the unfrozen dispersion; that is, the region close to the tip of the freezing front is more concentrated than that in the interior of the reaction system. After a critical concentration is reached, the unfrozen highly concentrated particle dispersion close to the freezing front resists further concentration so that the particles are no longer pushed by the freezing front. This results in the breakage of the solid/liquid interface and encapsulation of the particles in the frozen cyclohexane. The critical concentration at which the freezing front breaks depends on the concentration of the dispersion in the unfrozen region,<sup>33,34</sup> which, in turn, depends on the initial silica concentration. Thus, with increasing concentration of the silica nanoparticles, the size of the frozen domains in the reaction system becomes smaller so that the pore size of the final cryogel network decreases.

We have to mention that the freezing point of cyclohexane, when it is contained in the matrix of a porous solid, is strongly affected by the pore dimensions.<sup>35</sup> Recent measurements showed

(33) Uhlmann, D. R.; Chalmers, B.; Jackson, K. A. *J. Appl. Phys.* **1964**, *35*, 2986.

(34) Shanti, N. O.; Araki, K.; Halloran, J. W. *J. Am. Ceram. Soc.* **2006**, *89*, 2444.

(35) Mu, R.; Malhotra, V. M. *Phys. Rev. B* **1991**, *44*, 4296.

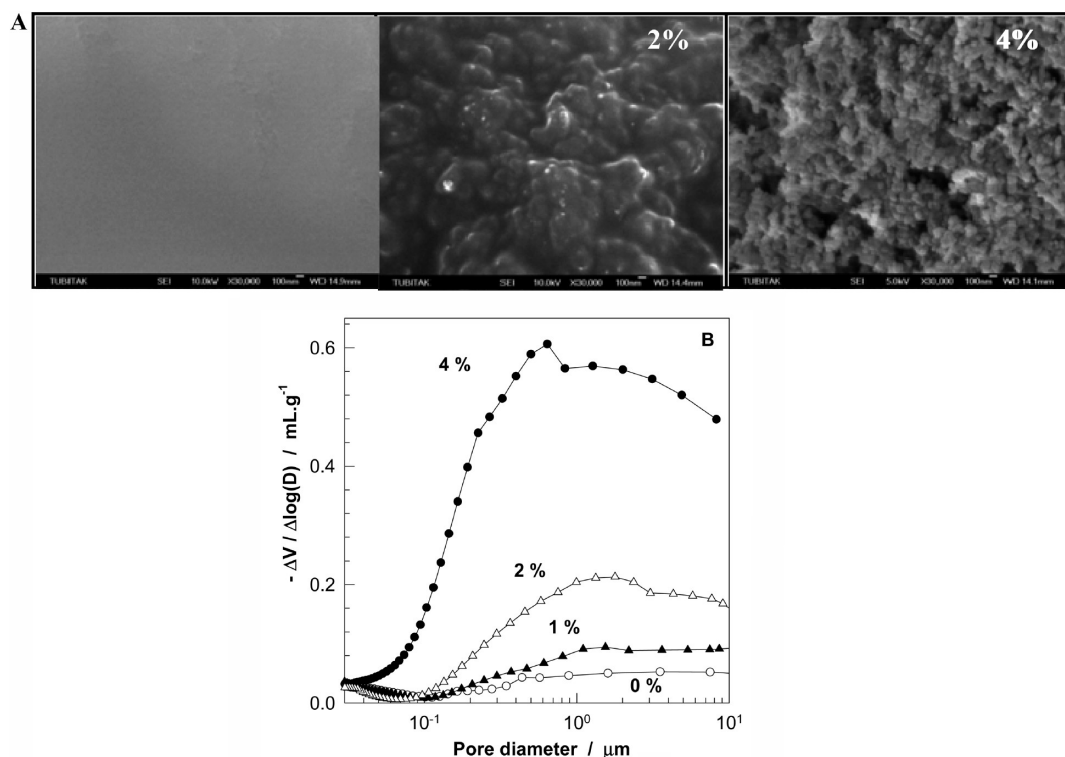


**Figure 6.** SEM images (A) and differential pore size distributions (B) of gel networks formed at  $-18\text{ }^{\circ}\text{C}$  with various amount of silica particles indicated. Scale bars in (A) are 100 nm.

that the degree of the suppression in the freezing temperature of cyclohexane confined in a porous silica scales linearly with the inverse of the mean pore size.<sup>36</sup> For example, cyclohexane freezes at  $-4\text{ }^{\circ}\text{C}$  and  $-14\text{ }^{\circ}\text{C}$  in pores of 33 and 15 nm in diameter, respectively compared to its bulk freezing temperature of  $6\text{ }^{\circ}\text{C}$ .<sup>36</sup> Thus, since silica particles in cyclohexane form a volume filling three-dimensional physical network (Figures 1), and the distance between the silica units further decreases due to cryoconcentration, cyclohexane in the interstices of the agglomerated particles remains unfrozen during freezing of the reaction solution. However, the excess bulk cyclohexane outside of the agglomerates freezes and expels PIB chains together with the cross-linker molecules toward the unfrozen regions. This leads to segregation of the inorganic and organic components in the reaction system, in which silica network locates close to the frozen domains while the polymer chains are shifted toward the unfrozen domains. Although silica segregation from the polymer should result in samples with poor mechanical properties, the present hybrid gels exhibit improved mechanical performance (Figure 2A). This suggests that the silica nanoparticles are not completely segregated from the polymer. The fact that the particles cannot be extracted from the hybrid gels also indicates extensive entanglements between the silica network and the cross-linked polymeric matrix.

**D. Small Pores in Hybrid Gels.** The variation of the internal morphology of the silica domains inside the large pores is illustrated in Figure 6A using images taken under a high magnification focusing into the large pores. At a low silica content, the silica particles are more or less fused together and they are covered by polymer chains. Individual nanoparticles in the agglomerates forming a three-dimensional structure can be identified as the

amount of silica is increased from 0 to 4% (Supporting Information Figure S4).

Increasing visibility of the individual silica particles with increasing silica content can be explained with the simultaneous decrease in the number of polymer chains per particle. From the molecular weight of PIB and the diameter of the particles, it was calculated that the average number of PIB chains per particle decreases from 14 to 4 as the silica content is increased from 1 to 4%. Thus, at a low silica content, the particles are covered by the polymer chains and the osmotic pressure due to the depletion forces further compresses the particles against each other so that they cannot be individually detected. At a high silica content, individual nanoparticles grow into agglomerates, leaving void interstices of sizes  $10^{-1}$ – $10^0\text{ }\mu\text{m}$ , which are 1–2 orders of magnitude smaller than the large pores formed due to cryogelation. This is also supported by the mercury porosimetry measurements. Figure 6B shows differential size distribution of pores below  $10\text{ }\mu\text{m}$  in diameter in hybrid networks formed at  $T_{\text{prep}} = -18\text{ }^{\circ}\text{C}$ . As the trend seen in Figure 6A, the hybrid gel network contains, in addition to macropores, micrometer and submicrometer sized pores due to the interstices formed between the particles and their agglomerates. The total volume of pores of diameters below  $10\text{ }\mu\text{m}$  increases from 0.15 to 1.1 mL/g with increasing silica content from 0 to 4%. As the silica content is decreased, the number of these pores rapidly decreases due to the fusion of the particles, as demonstrated by the SEM images.

We have to note that the hybrid gels presented here can be converted, depending on the type of the post-treatment, into organogels or into silica networks. Experiments showed that the silica component of hybrid gels accumulated in the pores can be dissolved in 48% aqueous hydrofluoric acid (HF) leading to the formation of organogels with pores of  $10^1\text{ }\mu\text{m}$  in diameter. This is illustrated in the SEM images given in Figure 7 before (A) and after (B) HF treatment as well as in Supporting Information

(36) Amanuel, S.; Bauer, H.; Bonventre, P.; Lasher, D. J. *Phys. Chem. C* **2009**, *113*, 18983.

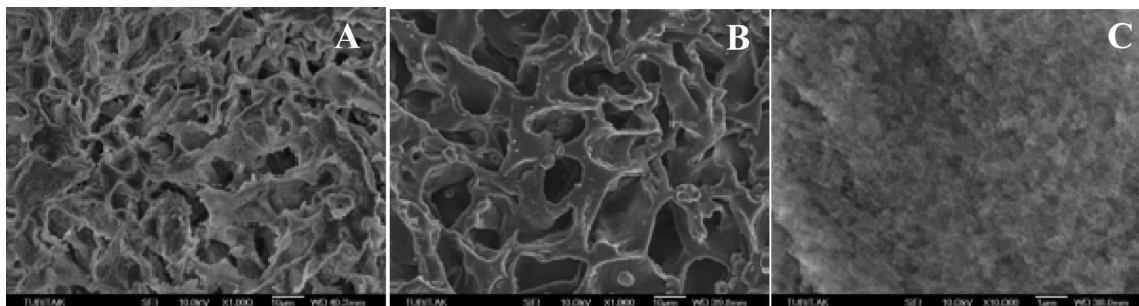


**Figure 7.** SEM images of hybrid gels before (A) and after (B) treatment with 48% HF, and after calcination (C). Gel preparation temperature =  $-18$  °C. Silica = 4%. Scaling bars are  $10\ \mu\text{m}$  (A, B) and  $1\ \mu\text{m}$  (C).

Figure S5. Further, removing the polymer component from the hybrid gel by calcination at  $600$  °C resulted in a porous silica network with  $10^{-1}\ \mu\text{m}$  sized pores, indicating that the morphology of the silica network in gels is retained after removing the polymer component (Figure 7C).<sup>37</sup> As seen in Figure 2, the silica network thus obtained has the same shape as the starting hybrid network.

### Conclusions

In recent years, organic–inorganic hybrid materials have attracted particular scientific and technological interest because of their excellent mechanical properties. Here, we described the preparation of a novel organic–inorganic hybrid cryogel consisting of cross-linked polyisobutylene chains and silica nanoparticles. The microstructure of the cryogels consists of two generations of pores:  $10^1\ \mu\text{m}$  sized large pores due to the cyclohexane crystals acting as a template during gelation, and  $10^{-1}$ – $10^0\ \mu\text{m}$  sized small pores between the aggregates of the silica nanoparticles. It was shown that the nanoparticles in hybrid cryogels accumulate within the large pores where cyclohexane crystals originally resided. Depending on the type of the post-treatment, hybrid cryogels can be converted into organic cryogels or into porous silica networks. Compared to the

(37) We have to note that the magnification of the SEM images after calcination was limited to  $\times 10\,000$  or below due to the contrast problem of the sample.

organogel networks with an elastic modulus of a few kPa, hybrid networks exhibit a modulus of elasticity around 300 kPa. We have to mention that, despite extensive efforts in the development of porous scaffolds with a good mechanical performance, all porous materials have an inherent lack of strength associated with porosity. The present macroporous hybrid gel networks exhibiting more than 1 order of magnitude higher modulus as compared to the conventional networks thus eliminate this shortcoming.

**Acknowledgment.** Work was supported by the Scientific and Technical Research Council of Turkey (TUBITAK), CAYDAG-107Y178. O.O. thanks Turkish Academy of Sciences (TUBA) for the partial support.

**Supporting Information Available:** Table S1 showing the silica content and the gel fraction of hybrid gel networks formed under various conditions, Figure S1 showing the mechanical spectra of PIB solutions containing silica particles, Figure S2 showing TG-DTG curves of a hybrid network formed at  $-18$  °C in the presence of 4% silica, Figures S3 and S4 showing SEM images of hybrid networks formed at  $-2$  and  $-18$  °C and at various silica contents, and Figure S5 showing SEM images of hybrid networks formed at  $-18$  °C after treatment with aqueous HF. This material is available free of charge via the Internet at <http://pubs.acs.org>.